HETEROCYCLES, Vol. 104, No. 10, 2022, pp. 1809 - 1821. © 2022 The Japan Institute of Heterocyclic Chemistry
Received, 22nd July, 2022, Accepted, 5th August, 2022, Published online, 19th August, 2022
DOI: 10.3987/COM-22-14725

DESIGN, SYNTHESIS, AND BIOLOGICAL ACTIVITY ANALYSIS OF NOVEL QUINAZOLINYL ETHER DERIVATIVES CONTAINING PIPERIDINAMIDE STRUCTURE

Peijia Li,[1,2] Yehui Yang,[2] Nan Wu,[2] Ya Yan,[2] Lian An,[2] Guangmin Tian,[2] and Xiaoping Bao[2]*

1 School of Chemistry and Chemical Engineering, Guizhou University, Guiyang 550025, People's Republic of China
2 State Key Laboratory Breeding Base of Green Pesticide and Agricultural Bioengineering, Key Laboratory of Green Pesticide and Agricultural Bioengineering, Ministry of Education, Centre for Research and Development of Fine Chemicals, Guizhou University, Guiyang 550025, People's Republic of China
***Corresponding author: Tel.: +86(0851)-88292090; Fax: +86(0851)-83622211; E-mail: Bxp800301@163.com

Abstract – We designed and synthesized 27 ether derivatives containing quinazolinyl piperidinamide structures and characterized them by ^{1}H NMR, ^{13}C NMR, and HRMS. Bioassay results indicate that several target compounds display higher inhibition activities *in vitro* against phytopathogenic bacteria. For example, the EC_{50} of compound **III-24** against *Xanthomonas axonopodis* pv. *citri* (*Xac*) is 33.9 μg/mL, which is double that of the commercialized bismerthiazol (EC_{50} = 75.5 μg/mL). Anti-*Xac* mechanisms show that compound **III-24** exerts antibacterial effects by increasing the permeability of bacterial membranes, reducing their exopolysaccharide content, and inducing morphological changes in bacterial cells.

INTRODUCTION

Agricultural production plays a crucial role in the survival and development of human beings. However, the production and quality of major food crops decline sharply every year because of plant diseases, which leads to large economic losses for farmers, and has become an important factor restricting the sustainable development of agriculture.[1] Most plant diseases are caused by phytobacteria.[2] The most

aggressive phytobacteria, *Xanthomonas axonopodis* pv. *citri* (*Xac*), is probably the most detrimental to citrus plants and extremely difficult to control in agricultural production.[3] It infects numerous important economic crops, such as citrus, kumquat, lemon, grapefruit, and wolfberry.[4,5] The pathogen *Xac* invades the mesophyll cell tissue of plants through stomata or wounds and colonizes the apoplasts of leaves, young stems, and fruits.[6,7] Presently, although there are excellent bactericides on the market, such as bismerthiazol and copper thiadiazole,[8] the drug resistance of pathogenic bacteria has been on the rise for a long time because of the unscientific use of bactericides, which has adverse effects on the environment.[9] Therefore, it is particularly urgent to find bactericides with novel structures and excellent properties that are environmentally friendly to solve the problem of drug resistance.[10]

Nitrogen-containing heterocyclic compounds have the characteristics of versatile biological activity, rich action sites, and diverse chemical structures. They have consistently played an important role in the research and synthesis of pesticides and medicine.[11,12] In the search for new drug-resistant bactericides and antibiotics, quinazoline and its derivatives exhibit numerous excellent properties, including antibacterial,[13] antiviral,[14] anti-inflammatory,[15] anticonvulsant,[16] antitumor,[17] antifungal,[18] and analgesic[19] activities. Currently listed quinazoline drugs include EGFR inhibitor PD153035, anticancer drug Erlotinib, acaricide Fenazaquin, and autophagy inhibitor Spautin-1 (Figure **1**). Therefore, quinazoline has attracted the extensive attention of numerous researchers. The quinazoline backbone is composed of two fused six-membered aromatic rings (namely, a benzene and a pyrimidine ring).[20] Because of its rich action points and derivatives with numerous excellent biological activities, it has a wide range of applications in the fields of medicine and pesticides. Taking quinazoline as the lead compound, the structural modification and transformation of its parent structure to design and synthesize quinazoline derivatives and screen their biological activities has become one of the research hotspots in the field of organic and medicinal chemistry.[21,22]

Piperidine group is an important pharmacophore, and piperidine derivatives possess a wide range of biological activities, including anticancer,[23] antivirals,[24] and antipsychotic[25] (Figure **1**). In our previous work,[9,26] we synthesized a small group of compounds containing piperidinyl quinazoline groups and evaluated their antibacterial and antifungal activities in agriculture. Notably, they showed good biological activity. As one of the most important classes of pesticides in the design and discovery of agrochemicals, formamide fungicides have been widely used worldwide because of their excellent fungicidal properties against highly destructive plant pathogens such as *Botrytis cinerea*, *Sclerotinia sclerotiorum*, and *Rhizoctonia solani*. Combining the advantages of the piperidine and amide groups, the piperidine amide group is used in the development of new pesticides for the first time.

Ether bonds in bioactive molecules have low cytotoxicity[27] and serve as favorable hydrogen bond acceptors. They have broad applications in drug discovery and development and are used in the antifungal

agent azoxystrobin, acaricidal pyrimidifen, insecticide pyriproxyfen, and herbicide oxyfluorfen (Figure **1**). Based on the above considerations, we designed and synthesized a series of novel quinazolinyl ether derivatives containing piperidinamide structures using a pharmacodynamic hybridization strategy (Figure **2**). We tested their antibacterial activities in vitro against three kinds of agriculturally important phytopathogenic bacteria. Finally, the antibacterial mechanisms of the high-activity compound were explored through experiments on the extracellular polysaccharide content, permeability of the bacterial membrane, and scanning electron microscope (SEM) observations.

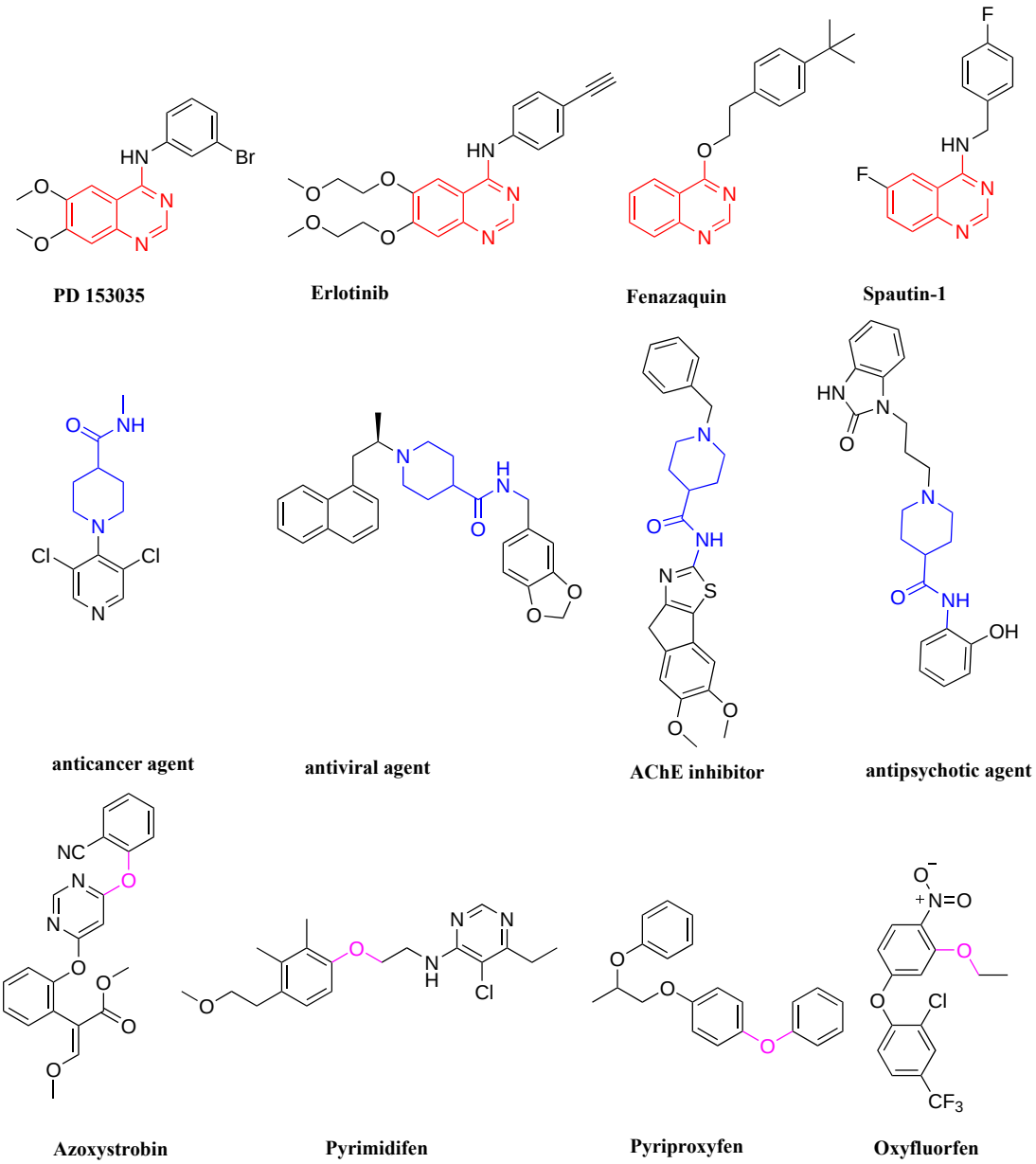

Figure 1. Selected examples of bioactive compounds containing the quinazoline, piperidinamide backbone, and ether bonds

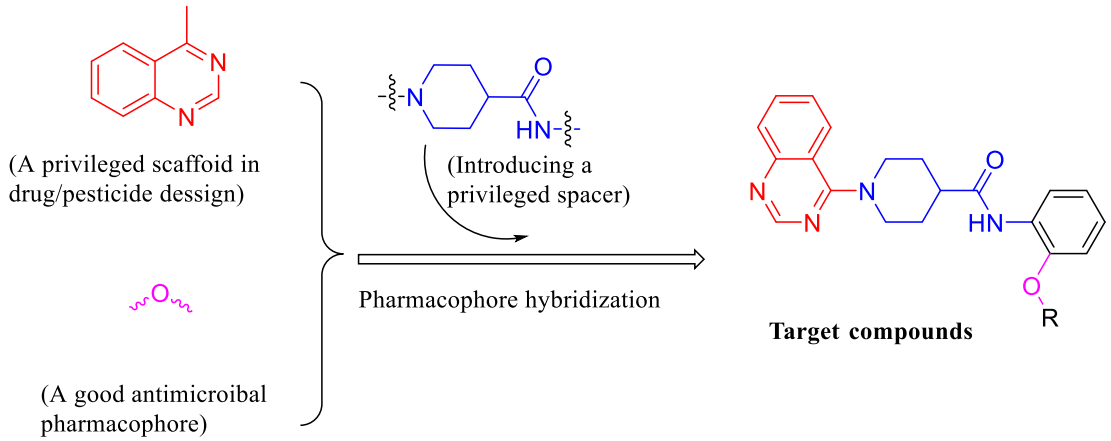

Figure 2. The design strategy of target compounds in this work

RESULTS AND DISCUSSION

Preparation of target compounds

As shown in Scheme **1**, target compounds **III-1**–**III-27** were synthesized in a continuous manner using quinazoline-modified piperidine carboxylic acid **1** as the starting material, which was prepared according to previously-reported procedures.[28] Briefly, acid **I** was chlorinated under the action of $SOCl_2$ to generate acid chloride. Subsequently, using tetrahydrofuran as a solvent and triethylamine as a catalyst, the acid chloride was directly reacted with 2-aminophenol to generate intermediate **II** with a yield of 47%. Finally, with acetonitrile as the solvent and potassium carbonate as an acid-binding agent, intermediate **II** reacts with halogenated compounds with different substituents to obtain target compounds **III-1**–**III-27**.

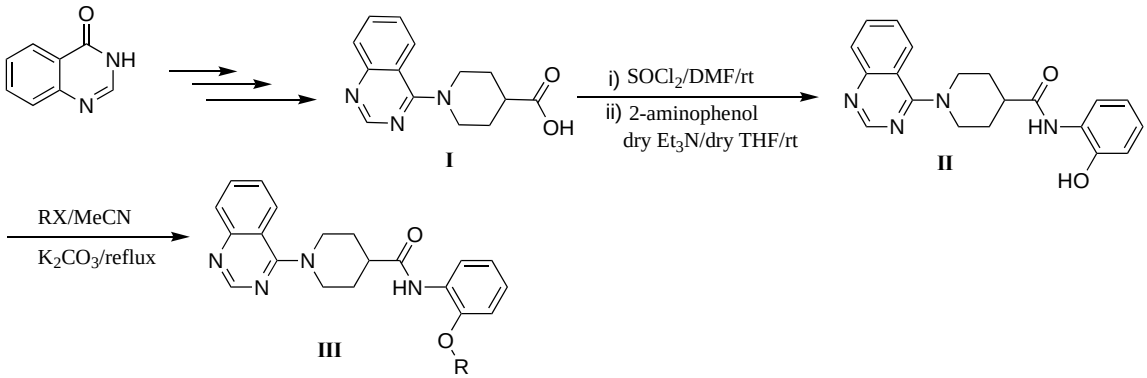

III-1:R = 2-CN-$C_6H_4CH_2$-
III-2:R = 3-CN-$C_6H_4CH_2$-
III-3:R = 4-CN-$C_6H_4CH_2$-
III-4:R = 2-Me-$C_6H_4CH_2$-
III-5:R = 3-Me-$C_6H_4CH_2$-
III-6:R = 4-Me-$C_6H_4CH_2$-
III-7:R = 2-F-$C_6H_4CH_2$-
III-8:R = 3-F-$C_6H_4CH_2$-
III-9:R = 4-F-$C_6H_4CH_2$-
III-10:R = 2-Cl-$C_6H_4CH_2$-
III-11:R = 3-Cl-$C_6H_4CH_2$-
III-12:R = 4-Cl-$C_6H_4CH_2$-
III-13:R = 2-CF_3-$C_6H_4CH_2$-
III-14:R = 2-OCF_3-$C_6H_4CH_2$-
III-15:R = 4-OCF_3-$C_6H_4CH_2$-
III-16:R = 4-^{t}Bu-$C_6H_4CH_2$-
III-17:R = 2,6-*di*-Cl-$C_6H_4CH_2$-
III-18:R = $PhCH_2$-
III-19:R = 2-OMe-$C_6H_4CH_2$-
III-20:R = Me-
III-21:R = Et-
III-22:R = Pr-
III-23:R = ^{n}Bu-
III-24:R = ^{s}Bu-
III-25:R = ^{i}Bu-
III-26:R = MeO_2CCH_2-
III-27:R = EtO_2CCH_2-

Scheme 1. Synthesis of target compounds **III-1–III-27**

Notably, apart from the purification of the target product by column chromatography, other intermediates only through simple filtration, washing, or recrystallization steps can be obtained in high yields. All target compounds were thoroughly characterized *via* ^{1}H NMR, ^{13}C NMR, and HRMS spectroscopic data.

Structural characterization of target compounds

The target compound was subjected to spectroscopic analysis, taking compound **III-18** as an example. In the ^{1}H NMR spectrum, the proton signal of NH of the amide of compound **III-18** is a single peak at δ = 9.18 ppm; the proton signal of the methine (CH) at position 2 of quinazoline is a single peak at δ = 8.63 ppm; the proton signals on the quinazoline ring and two benzene rings are concentrated between δ = 6.90–7.99; the proton signal of the methylene group (CH_2) of the benzyl group is singlet peak at δ = 5.20. δ = 1.85–1.96 ppm, δ = 3.19–3.24 ppm, and δ = 4.30–4.33 ppm denote the methylene (CH_2) proton signal peak on the piperidine ring. δ = 2.86–2.89 represents the upper methine (CH) proton signal peak of the piperidine ring. In the ^{13}C NMR spectrum, the methine signals of the three-carbon and ether bonds on the piperidine ring appear in the high field, and the carbon signals of the aromatic and amides appear in the relatively low field. In the HRMS-ESI spectrum, compound **III-18** exhibits a strong quasimolecular ion peak $[M + H]^{+}$, and the measured value is consistent with the theoretical calculation, which further confirms the structure of the target compound.

***In vitro* antibacterial activity**

The turbidimetric method[26,29] was used to assess *in vitro* antibacterial activity of compounds **III-1**–**III-27** against three types of plant pathogenic bacteria *Xanthomonas oryzae* pv. *oryzae* (*Xoo*), *Xanthomonas axonopodis* pv. *citri* (*Xac*), and *Pseudomonas syringae* pv. *actinidiae* (*Psa*), with commercialized bactericide bismerthiazol (BMT) as the positive control agent. Table **1** indicates that several compounds exhibit good antibacterial effects against the tested bacteria. For example, four compounds (including **III-3**, **III-10**, **III-19**, and **III-26)** had inhibitory rates of 50.7%–57.5% against *Xoo* at 100 μg/mL, similar to the control BMT (53.8%). Moreover, the inhibitory rate of compound **III-24** on *Xac* was 85.4%, which is substantially higher than that of the positive control drug BMT (54.0%).

Encouraged by preliminary antibacterial results, EC_{50} values (half-maximal effective concentration) of several compounds against the bacteria *Xac* were subsequently measured using the serial dilution method.[28] As shown in Table **2**, compound **III-24** exhibited an EC_{50} value of 33.9 μg/mL against *Xac*, which is considerably lower than that of control BMT (75.5 μg/mL). Furthermore, compounds **III-2** and **III-22** had EC_{50} values of 86.1 and 84.6 μg/mL against *Xac*, respectively, similar to control BMT.

Table 1. Antibacterial Activities of Target Compounds **III-1**–**III-27** against four Phytopathogenic Bacteria *Xoo*, *Xac*, and *Psa in Vitro*

Compd.	Inhibition rate[a] (%)					
	Xoo		*Xac*		*Psa*	
	100 μg/mL	50 μg/mL	100 μg/mL	50 μg/mL	100 μg/mL	50 μg/mL
III-1	18.6 ± 2.4	13.0 ± 2.5	22.0 ± 1.3	7.9 ± 1.6	22.8 ± 1.1	18.1 ± 2.4
III-2	40.3 ± 2.1	36.0 ± 2.5	53.3 ± 2.7	35.3 ± 2.8	35.0 ± 3.1	33.9 ± 2.5
III-3	55.7 ± 5.2	17.3 ± 4.4	11.0 ± 0.8	0	39.0 ± 1.1	26.2 ± 3.8
III-4	20.2 ± 1.3	16.3 ± 2.6	25.5 ± 5.2	5.5 ± 3.1	23.6 ± 3.7	21.7 ± 4.1
III-5	26.3 ± 3.1	25.2 ± 3.0	18.2 ± 2.3	17.2 ± 3.9	20.6 ± 1.3	18.4 ± 1.0
III-6	43.6 ± 2.2	34.0 ± 2.3	22.0 ± 3.0	12.4 ± 3.4	38.1 ± 2.0	28.3 ± 2.4
III-7	43.5 ± 1.7	30.4 ± 8.9	22.5 ± 1.8	0	41.7 ± 0.0	27.8 ± 1.2
III-8	43.6 ± 3.5	30.0 ± 4.4	11.1 ± 2.0	0	32.7 ± 0.9	26.4 ± 1.8
III-9	30.1 ± 1.1	17.5 ± 2.3	15.1 ± 5.7	7.8 ± 4.5	16.3 ± 1.2	11.4 ± 1.3
III-10	57.5 ± 1.9	45.3 ± 0.5	14.6 ± 5.7	12.4 ± 3.4	35.2 ± 1.1	23.0 ± 1.6
III-11	39.4 ± 1.2	28.8 ± 4.4	15.8 ± 1.9	0	41.4 ± 1.6	35.5 ± 2.6
III-12	41.3 ± 2.4	26.3 ± 3.6	13.1 ± 5.9	14.2 ± 1.3	24.7 ± 0.9	13.6 ± 2.0
III-13	38.2 ± 5.2	14.4 ± 7.0	24.2 ± 5.5	15.6 ± 4.1	26.5 ± 1.7	18.2 ± 0.4
III-14	30.1 ± 3.1	26.8 ± 3.3	11.6 ± 2.0	0	30.2 ± 1.0	6.8 ± 3.2
III-15	31.2 ± 3.0	19.3 ± 6.3	14.4 ± 3.3	8.0 ± 1.4	34.3 ± 0.8	33.9 ± 2.5
III-16	29.8 ± 3.4	0	18.3 ± 1.6	13.0 ± 1.2	20.8 ± 1.9	15.2 ± 1.6
III-17	31.8 ± 3.0	17.1 ± 8.5	49.6 ± 2.2	22.0 ± 2.0	38.5 ± 2.8	17.5 ± 2.3
III-18	36.1 ± 3.0	7.9 ± 3.6	19.6 ± 2.0	8.6 ± 2.1	12.0 ± 1.8	21.9 ± 1.1
III-19	50.7 ± 2.7	19.9 ± 4.9	17.5 ± 2.4	8.5 ± 3.0	26.6 ± 7.5	16.4 ± 1.0
III-20	18.4 ± 5.3	10.6 ± 0.6	35.9 ± 1.3	16.6 ± 2.8	18.2 ± 2.0	12.7 ± 1.6
III-21	44.6 ± 1.5	29.5 ± 3.0	15.9 ± 0.8	7.0 ± 2.5	32.6 ± 4.6	20.1 ± 2.6
III-22	38.1 ± 3.5	26.5 ± 4.3	48.2 ± 2.2	42.4 ± 1.1	21.6 ± 3.0	17.0 ± 0.5
III-23	45.2 ± 1.7	19.7 ± 3.1	33.7 ± 1.5	19.3 ± 1.5	16.7 ± 0.5	19.3 ± 1.7
III-24	26.6 ± 2.7	23.1 ± 4.6	85.4 ± 3.2	71.3 ± 4.2	40.7 ± 1.8	22.1 ± 2.8
III-25	12.0 ± 1.3	17.2 ± 5.1	47.1 ± 0.4	18.6 ± 2.3	20.2 ± 2.1	0
III-26	56.7 ± 1.7	27.7 ± 4.9	28.8 ± 0.7	10.4 ± 1.4	57.3 ± 1.5	26.5 ± 1.5
III-27	16.5 ± 5.7	6.6 ± 2.6	37.7 ± 1.7	10.0 ± 1.5	14.1 ± 2.8	13.6 ± 0.5
BMT[b]	53.8 ± 3.0	30.4 ± 2.8	54.0 ± 0.4	37.9 ± 2.0	50.0 ± 1.2	39.4 ± 1.5

[a] The average of three trials. [b] The agrobactericide bismerthiazol (BMT) was used as a positive control agent.

Table 2. The EC_{50} values of some compounds against *Xac*

Compd.	Bacteria	Toxic regression equation	*r*	EC_{50}[a] (μg/mL)
III-2	*Xac*	$y = 1.1629x + 2.7496$	0.9856	86.1 ± 11.1
III-22	*Xac*	$y = 1.0112x + 3.0508$	0.9655	84.6 ± 9.1
III-24	*Xac*	$y = 1.5505x + 2.6265$	0.9877	33.9 ± 3.4
BMT[b]	*Xac*	$y = 1.3038x + 2.5515$	0.9889	75.5 ± 2.3

[a] Average of three replicates; [b] The commercial antibacterial agent bismerthiazol (BMT) was used as a positive control.

Effect on extracellular polysaccharide production of compound III-24

Bacterial extracellular polysaccharides (EPS) not only are involved in bacterial film formation but also function as important virulence factors for numerous bacterial pathogens.[26,30,31] Thus, the influence of high-activity compound **III-24** on the content of EPS of the *Xac* was subsequently tested (Figure **3**). When *Xac* was treated with compound **III-24** at concentrations of 25, 50, and 100 μg/mL, the corresponding extracellular polysaccharide productions were reduced by 19.2%, 31.7%, and 55.9%,

respectively, in comparison with the negative control. This finding indicates that compound **III-24** is capable of generating a remarkable inhibition effect on the *Xac* production of EPS.

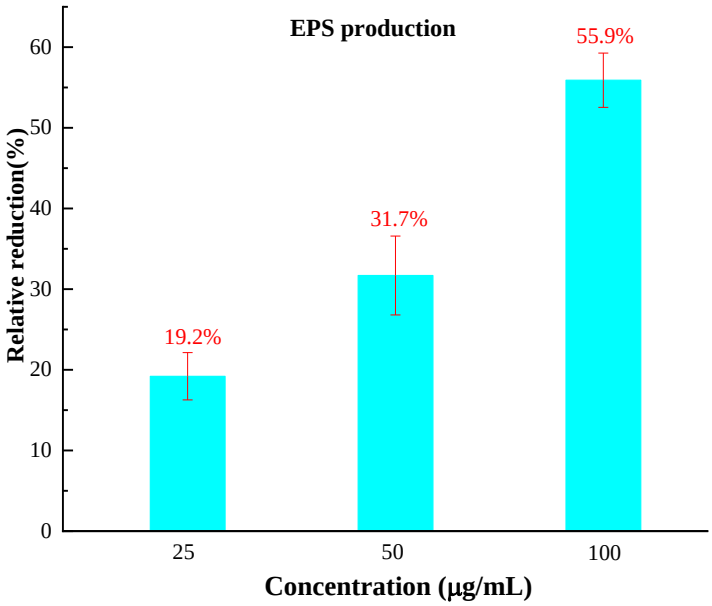

Figure 3. Changes in the extracellular polysaccharide production of the *Xac* after treatment with compound **III-24** at different concentrations

Effect on bacterial membrane permeability of compound III-24

Numerous antibiotics exert their antibacterial effects by altering the cell membrane permeability of bacteria.[26,30] Therefore, we evaluated the antibacterial activity of compound **III-24** by studying the relative permeability of compound **III-24** to *Xac*. Figure **4** shows the results of the treatment of *Xac* with

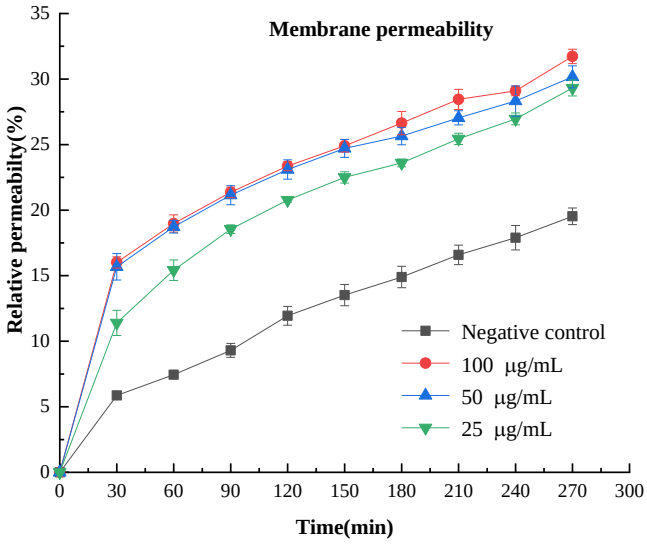

Figure 4. Changes in the membrane permeability of the pathogen *Xac* after treatment with compound **III-24** at different concentrations

compound **III-24** at concentrations of 25, 50, and 100 μg/mL. The relative permeability of the *Xac* membrane increases with the increasing concentrations of compound **III-24** and longer treatment time. Particularly between 30 and 120 min, the growth rate was faster, and all were higher than the negative control. This indicates that compound **III-24** could exert an antibacterial effect by changing the permeability of the *Xac* cell membrane.

SEM studies on cell morphology

The morphological difference analysis of the cell structure of *Xac* treated with the compound **III-24**,[27,28] exhibiting the best antibacterial activity, was conducted via the SEM. Figure **5** shows the results. The shape of the bacteria *Xac* in the control group is plump and smooth (Figure **5A**). After treatment with 100 μg/mL **III-24**, *Xac* cells were deformed, shriveled, or even damaged (Figure **5B**). When the concentration of **III-24** was increased to 200 μg/mL, the cell membrane damage of *Xac* bacteria increased (Figure **5C**). Based on the above SEM results of *Xac*, **III-24** achieves the bacteriostatic effect by altering its cell morphology.

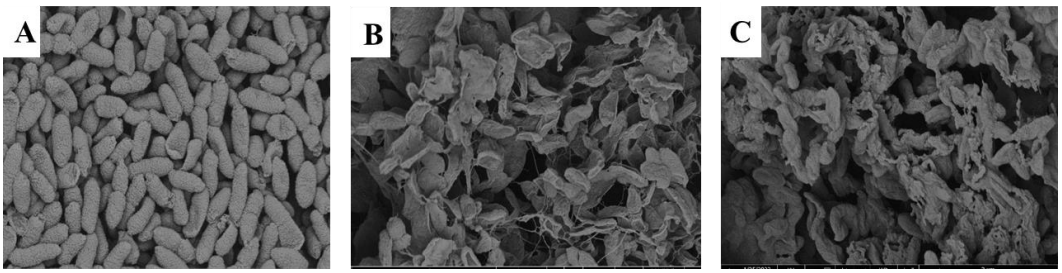

Figure 5. SEM images for the changes in the cell morphologies of *Xac* after treatment with compound **III-24** at different concentrations: **A**) 0, **B**) 100, and **C**) 200 μg/mL (scale bar: 3.0 μm)

CONCLUSIONS

We designed and synthesized a series of novel quinazoline ether derivatives containing piperidinamide moieties as agricultural antibacterial agents. *In vitro* antibacterial assays indicate that compound **III-24** exhibits significantly better bactericidal activity against *Xac* than the control bismerthiazol. The study of anti-*Xac* mechanisms shows that compound **III-24** exerts antibacterial effects by increasing the permeability of bacterial membranes, reducing the content of exopolysaccharides, and inducing morphological changes in bacterial cells.

EXPERIMENTAL

General

Melting points were measured on an XT-4 binocular microscope (Beijing Tech Instrument, China) and uncorrected. ^{1}H and ^{13}C NMR spectra were collected on a Bruker Avance III 400 MHz NMR

spectrometer at 298 K using DMSO-d_6 as a solvent and TMS as an internal standard, and chemical shift (δ) was expressed in parts per million (ppm). The following abbreviations were employed in expressing the multiplicity: s = singlet, d = doublet, t = triplet, q = quartet, m = multiplet. High-resolution mass spectra (HRMS) were determined on a Thermo Scientific Q Exactify Hybrid Quadrupole-Orbitrap mass spectrometer. SEM images were visualized and obtained using a Nova NanoSEM 450. The conductivities were determined on an electrical conductivity meter DDS-307. All the chemicals were purchased from commercial suppliers and directly used without further purification (unless stated otherwise).

Synthesis of intermediate II

Acid **I** (258 mg, 1.00 mmol) and 0.5 mL of dimethylformamide (DMF) were added to $SOCl_2$ (15 mL) solution. The above mixture was stirred at room temperature for 8 h. Then, excess $SOCl_2$ was removed under reduced pressure to generate acid chloride, which was added together with 2-aminophenol (109 mg, 1.00 mmol) into anhydrous tetrahydrofuran (THF, 20 mL) using anhydrous triethylamine (2 mL) as a catalyst. The mixture was then stirred at room temperature for 6 h. The solution after the above reaction was directly poured into water, stirred overnight, and then filtered with suction to obtain the intermediate **II**.

***N*-(2-Hydroxyphenyl)-1-(quinazolin-4-yl)piperidine-4-carboxamide (II)** (**II**): red solid, Yield: 47%, mp 256–257 °C.^{1}H NMR (400 MHz, DMSO-d_6) δ: 9.80 (s, 1H), 9.29 (s, 1H), 8.63 (s, 1H), 8.00 (d, J = 8.4 Hz, 1H), 7.81–7.80 (m, 2H), 7.75 (d, J = 8.0 Hz, 1H), 7.58–7.51 (m, 1H), 6.95–6.92 (m, 1H), 6.86 (d, J = 8.1 Hz, 1H), 6.78–6.74 (m, 1H), 4.34 (d, J = 14.3 Hz, 2H), 3.20 (t, J = 12.8 Hz, 2H), 2.95–2.86 (m, 1H), 1.95 (d, J = 12.1 Hz, 2H), 1.91–1.81 (m, 2H). ^{13}C NMR (100 MHz, DMSO-d_6) δ: 173.6, 164.0, 153.8, 151.4, 148.0, 132.8, 128.1, 126.4, 125.7, 125.5, 124.7, 122.4, 119.1, 116.0, 115.8, 49.1, 42.3, 28.6. ESI-HRMS *m/z*: $[M - H]^-$ calcd for $C_{20}H_{19}N_4O_2$: 347.1503; found: 347.1514.

General procedures for the synthesis of target compounds III-1–III-28

Intermediate **II** (350 mg, 1.00 mmol), 1.2 equivalents of benzenesulfonyl chloride, and catalyst triethylamine (0.5 mL) were added to the acetonitrile solution. The mixture was stirred at room temperature for 8 h. After completion, monitored via thin-layer chromatography, purification by column chromatography (with 2: 1 EtOAc/CH_2Cl_2) yielded target compounds **III-1–III-27**.

***N*-[2-[(2-Cyanobenzyl)oxy]phenyl]-1-(quinazolin-4-yl)piperidine-4-carboxamide** (**III-1**): White solid, mp 219–220 °C, yield: 43.6%. ^{1}H NMR (400 MHz, DMSO-d_6) δ: 9.07 (s, 1H), 8.63 (s, 1H), 7.97 (d, J = 8.2 Hz, 1H), 7.90 (d, J = 6.5 Hz, 1H), 7.86 (d, J = 6.2 Hz, 1H), 7.81–7.79 (m, 2H), 7.78 (s, 1H), 7.76–7.72 (m, 1H), 7.57–7.52 (m, 2H), 7.17–7.07 (m, 2H), 6.98–6.94 (m, 1H) , 5.35 (s, 2H), 4.30 (d, J = 13.3 Hz, 2H), 3.20 (t, J = 11.1 Hz, 2H), 2.91–2.79 (m, 1H), 1.94 (d, J = 9.4 Hz, 2H), 1.91–1.79 (m, 2H).

^{13}C NMR (100 MHz, DMSO) δ: 173.1, 163.9, 153.6, 151.2, 148.9, 140.1, 133.5, 133.3, 132.8, 129.5, 129.1, 127.9, 127.8, 125.7, 125.4, 124.7, 123.3, 121.2, 117.5, 115.9, 113.1, 110.9, 68.1, 48.9, 42.3, 28.4. ESI-HRMS *m/z*: $[M + H]^+$ calcd for: $C_{28}H_{26}O_2N_5$: 464.2081; found: 464.2079.

In vitro antibacterial bioassay

The in vitro antibacterial effects of target compounds **III-1** to **III-27** against three plant pathogens *Xoo*, *Xac*, and *Psa* at concentrations of 100 and 50 μg/mL were determined by the classical turbidimetric method.[26,29] Pure DMSO in sterile distilled water was employed as blank control, and commercially available agrobactericide BMT was used as a positive control agent. About 40 μL of solvent NB (3.0 g of beef extract, 5.0 g of peptone, 1.0 g of yeast powder, 10.0 g of glucose, 1000 mL of distilled water, pH 7.0–7.2) containing the bacterium *Xoo*, *Xac* or *Psa* was added to a mixed solvent system comprising 4 mL of solvent NB and 1 mL of 0.1% Tween-20 containing tested compound or BMT. The above test tubes were incubated at 28 ± 1 °C and continuously shaken at 180 rpm for one to three days. The bacterial growth was monitored by measuring the optical density at 595 nm (OD_{595}), given by the $\text{turbidity}_{\text{corrected values}} = OD_{\text{bacterium}} - OD_{\text{no bacterium}}$ and $I = (C_{\text{tur}} - T_{\text{tur}})/C_{\text{tur}} \times 100\%$. The C_{tur} represents the corrected turbidity value of bacterial growth of untreated NB (blank control), and T_{tur} represents the corrected turbidity value of bacterial growth of tested compound-treated NB. Finally, I denote the inhibition ratio of the tested compound against this bacterium.

Next, the target compounds that showed good bactericidal activity in the primary screening were further tested for their antibacterial activities against pathogenic *Xac* at 5 different concentrations (namely 100, 50, 25, 12.5, and 6.25 μg/mL), and then they obtained the EC_{50} value of SPSS 17.0 software was used for probabilistic analysis.[26]

EPS production

The effect of compound **III-24** on the production of extracellular polysaccharides of *Xac* was measured using the previous methods.[26,30,31] The *Xac* cultures were treated with compound **III-24** at different concentrations of 25, 50, and 100 μg/mL, respectively. The same treatment with an equivalent volume of DMSO as the negative control. Next, the above cultures were incubated for 72 h at 28 °C with shaking at 180 rpm. Subsequently, the supernatant was gathered by centrifugation, and EPS was precipitated by adding EtOH (60 mL) and allowed to stand overnight. Finally, the formed EPS precipitates were collected by centrifugation and dried at 70 °C.

Membrane permeability

Bacterial membrane permeability was measured using the previously reported methods.[28,30] Briefly, 20 mL of *Xac* cultures were centrifuged at 2000 rpm for 20 min to remove the medium and the cells were

collected. The cells were washed and re-suspended with 20 mL sterile water. Subsequently, the cells were treated with compound **III-24** or control BMT at different concentrations of 25, 50, and 100 μg/mL, respectively. There is the same treatment with an equivalent volume of DMSO as a negative control. The conductivities of bacterial suspension at 0, 30, 60, 90, 120, 150, 180, 210, 240, 270, and 300 min were recorded, respectively. Finally, the culture was boiled for 10 min to kill the pathogen *Xac*, and this conductivity was also recorded. The relative permeability P was calculated using the following formula:

$$P = (C_t - C_0)/(C_k - C_0) \times 100\%$$

where C_0 is the conductivity at 0 min, C_t is the conductivity at different periods, and C_k is the conductivity after killing *Xac*.

Scanning electron microscopy observation[26,29]

A 1.5 mL of *Xac* cell suspension within the logarithmic growth phase was centrifuged and washed with PBS buffer (pH = 7.2) three times and then re-suspended with 1.5 mL PBS buffer. Next, these *Xac* cells were incubated with compound **III-24** at two concentrations of 200 and 100 μg/mL for 8 ~ 10 h, respectively. At the same time, an equi-volume of DMSO was also employed as the blank control. After that, these samples were washed three times with PBS buffer (pH = 7.2). Next, these *Xac* cells were immobilized using 2.5% glutaraldehyde solution for 8 h at 4 °C, followed by dehydration with graded ethanol solution and absolute *tert*-butanol, respectively. Eventually, these samples were freezedried, coated with gold, and visualized by use of a Nova NanoSEM 450 instrument.

ACKNOWLEDGEMENTS

This work was financially supported by the National Natural Science Foundation of China (No. 32060626) and Natural Science Foundation of Guizhou Province (No. 20201Z025).

SUPPORTING INFORMATION

Characterization data and original spectral files for all the intermediates and target compounds (including ^{1}H, ^{13}C NMR and HRMS) are in Supporting Information file.

Conflict of interest

The authors declare no competing financial interest.

REFERENCES AND NOTES

1. K. Kazan and D. M. Gardiner, *Mol. Plant Pathol.*, 2018, **19**, 1547.
2. X. Q. Yu, X. Y. Zhu, Y. Zhou, Q. L. Li, Z. Hu, T. Li, J. Tao, M. L. Dou, M. Zhang, Y. Shao, and R.

F. Sun, *J. Agric. Food Chem.*, 2019, **67**, 13904.

3. L. M. Moreira, M. R. Soares, A. P. Facincani, C. B. Ferreira, R. M. Ferreira, M. L. T. Ferro, F. C. Gozzo, É. B. Felestrino, R. A. B. Assis, C. C. M. Garcia, J. C. Setubal, J. A. Ferro, and J. C. F. Oliveira, *BMC Microbiol.*, 2017, **17**, 155.
4. R. A. Cernadas, L. R. Camillo, and C. E. Benedetti, *Mol. Plant Pathol.*, 2008, **9**, 609.
5. C. M. Carnielli, J. Artier, J. C. F. Oliveira, and M. T. M. Novo-Mansur, *J. Proteomics*, 2017, **151**, 251.
6. J. H. Graham, T. R. Gottwald, J. Cubero, and D. S. Achor, *Mol. Plant Pathol.*, 2004, **5**, 1.
7. T. Zimaro, L. Thomas, C. Marondedze, B. S. Garavaglia, C. Gehring, J. Ottado, and N. Gottig, *BMC Microbiol.*, 2013, **13**, 186.
8. X. M. Tang, Q. Zhou, W. L. Zhan, D. Hu, R. Zhou, N. Sun, S. Chen, W. N. Wu, and X. Wei, *RSC Adv.*, 2022, **12**, 2399.
9. J. Shi, M. H. Ding, N. Luo, S. R. Wang, P. J. Li, J. H. Li, and X. P. Bao, *J. Agric. Food Chem.*, 2020, **68**, 9613.
10. D. Y. Liu, J. Zhang, L. Zhao, W. J. He, Z. J. Liu, X. H. Gan, and B. A. Song, *J. Agric. Food Chem.*, 2019, **67**, 11860.
11. B. Yu, S. Zhou, L. X. Cao, Z. S. Hao, D. Y. Yang, X. F. Gou, N. L. Zhang, V. A. Bakulev, and Z. J. Fan, *J. Agric. Food Chem.*, 2020, **68**, 7093.
12. M. W. Wang, H. H. Zhu, P. Y. Wang, D. Zeng, Y. Y. Wu, L. W. Liu, Z. B. Wu, Z. Li, and S. Yang, *J. Agric. Food Chem.*, 2019, **67**, 12696.
13. Q. S. Long, L. W. Liu, Y. L. Zhao, P. Y. Wang, B. Chen, Z. Li, and S. Yang, *J. Agric. Food Chem.*, 2019, **67**, 11005.
14. D. D. Xie, J. Shi, A. W. Zhang, Z. W. Lei, G. C. Zu, Y. Fu, X. H. Gan, L. M. Yin, B. A. Song, and D. Y. Hu, *Bioorg. Chem.*, 2018, **80**, 433.
15. A. M. Alafeefy, A. A. Kadi, O. A. Al-Deeb, K. E. H. El-Tahir, and N. A. Al-jaber, *Eur. J. Med. Chem.*, 2010, **45**, 4947.
16. H. M. Patel, M. Noolvi, A. Shirkhedkar, A. Kulkarni, C. V. Pardeshi, and S. Surana, *RSC Adv.*, 2016, **6**, 44435.
17. R. Pérez-Soler, A. Chachoua, L. A. Hammond, E. K. Rowinsky, M. Huberman, D. Karp, J. Rigas, G. M. Clark, P. Santabárbara, and P. Bonomi, *J. Clin. Oncol.*, 2004, **22**, 3238.
18. W. J. Li, Q. Li, D. L. Liu, and M. W. Ding, *J. Agric. Food Chem.*, 2013, **61**, 1419.
19. A. B. A. El-Gazzar, M. M. Youssef, A. M. S. Youssef, A. A. Abu-Hashem, and F. A. Badria, *Eur. J. Med. Chem.*, 2009, **44**, 609.
20. R. Bansal and A. Malhotra, *Eur. J. Med. Chem.*, 2021, **211**, 113036.

21. M. Faisal and A. Saeed, *Front. Chem.*, 2021, **8**, 594717.
22. V. Alagarsamy, K. Chitra, G. Saravanan, V. Raja Solomon, M. T. Sulthan, and B. Narendhar, *Eur. J. Med. Chem.*, 2018, **151**, 628.
23. A. Mallinger, S. Crumpler, M. Pichowicz, D. Waalboer, M. Stubbs, O. Adeniji-Popoola, B. Wood, E. Smith, C. Thai, A. T. Henley, K. Georgi, W. Court, S. Hobbs, G. Box, M.-J. Ortiz-Ruiz, M. Valenti, A. D. H. Brandon, R. TePoele, B. Leuthner, P. Workman, W. Aherne, O. Poeschke, T. Dale, D. Wienke, C. Esdar, F. Rohdich, F. Raynaud, P. A. Clarke, S. A. Eccles, F. Stieber, K. Schiemann, and J. Blagg, *J. Med. Chem.*, 2015, **58**, 1717.
24. A. K. Ghosh, J. Takayama, K. V. Rao, K. Ratia, R. Chaudhuri, D. C. Mulhearn, H. Lee, D. B. Nichols, S. Baliji, S. C. Baker, M. E. Johnson, and A. D. Mesecar, *J. Med. Chem.*, 2010, **53**, 4968.
25. A. A. Kaczor, K. M. Targowska-Duda, A. G. Silva, M. Kondej, G. Biała, and M. Castro, *Biomolecules*, 2020, **10**, 349.
26. M. H. Ding, S. R. Wang, N. Wu, Y. Yan, J. H. Li, and X. P. Bao, *J. Agric. Food Chem.*, 2021, **69**, 15084.
27. J. Tong, Y. Wu, and M. Bai, *J. Struct. Chem.*, 2018, **59**, 1564.
28. R. Krishnathas, E. Bonke, S. Dröse, V. Zickermann, and H. R. Nasiri, *Med. Chem. Commun.*, 2017, **8**, 657.
29. J. Shi, N. Luo, M. H. Ding, C. H. Li, S. R. Wang, P. J. Li, J. H. Li, and X. P. Bao, *Chin. J. Org. Chem.*, 2021, **41**, 738.
30. C. Q. Wei, J. J. Huang, Y. Q. Luo, S. B. Wang, S. K. Wu, Z. F. Xing, and J. X. Chen, *Pestic. Biochem. Physiol.*, 2021, **175**, 104857.
31. C. F. Yi, J. X. Chen, C. Q. Wei, S. K. Wu, S. B. Wang, D. Y. Hu, and B. A. Song, *Bioorg. Med. Chem. Lett.*, 2020, **30**, 126814.